Published in final edited form as:

ACS Chem Biol. 2022 November 18; 17(11): 3047–3058. doi:10.1021/acschembio.1c00906.

Structure Guided Design of Bacteriophage Qβ Mutants as Next Generation Carriers for Conjugate Vaccines

Suttipun Sungsuwan,
Department of Chemistry, Michigan State University, East Lansing, Michigan 48824, United States

Virology and Cell Technology Research Team, National Center for Genetic Engineering and Biotechnology (BIOTEC), National Science and Technology Development Agency (NSTDA), Pathum Thani 12120, Thailand

Xuanjun Wu,
Department of Chemistry and Institute for Quantitative Health Science and Engineering, Michigan State University, East Lansing, Michigan 48824, United States

National Glycoengineering Research Center, Shandong Key Laboratory of Carbohydrate Chemistry and Glycobiology, Shandong University, Qingdao, Shandong 266237, China

Vincent Shaw,
Department of Chemistry, Michigan State University, East Lansing, Michigan 48824, United States

Herbert Kavunja,
Iaso Therapeutics Inc., East Lansing, Michigan 48823, United States

Hunter McFall-Boegeman,
Department of Chemistry and Institute for Quantitative Health Science and Engineering, Michigan State University, East Lansing, Michigan 48824, United States

Zahra Rashidijahanabad,

Corresponding Authors: Xiangshu Jin – Department of Chemistry, Michigan State University, East Lansing, Michigan 48824, United States; jinxiang@msu.edu, **Xuefei Huang** – Department of Chemistry, Institute for Quantitative Health Science and Engineering, and Department of Biomedical Engineering, Michigan State University, East Lansing, Michigan 48824, United States; huangxu2@msu.edu.

Author Contributions

S.S., X.H., and X.W. designed the project. S.S., X.W., Z.Y., Z.T., and S.R. expressed the mutants and synthesized the conjugates. S.S., X.W., H.K., H.M., L.S., Z.T., S.N., P.L., and Z.R. performed the animal studies. V.S. and X.J. performed the structural studies. All authors contributed to the preparation of the manuscript.

Supporting Information

The Supporting Information is available free of charge at https://pubs.acs.org/doi/10.1021/acschembio.1c00906.
Synthesis and characterization of Tn1, wtQβ, or mQβ conjugates and CRM197-Tn, tetanus toxoid-Tn, and KLH-Tn conjugates; supplementary Figures S1–S7; MS spectra of Qβ-Tn; Qβ peptide sequences and ELISA; TEM images of wtQβ and various mQβ; SDS-PAGE analysis; stability analysis of Qβ; IgG subtype profiles; ELISA results of postimmunized sera; supplementary Tables S1 and S2, physical characteristics of wtQβ and primers used; procedures for size exclusion chromatography; site-directed mutagenesis of Qβ VLPs; accessible surface area measurement; ELISA; cell culture; flow cytometry experiment; SDS PAGE analysis; conjugation of GD2 and RBD peptide epitopes of mQβ; antitumor immunotherapy; NMR spectra; and supplementary references (PDF)

Complete contact information is available at: https://pubs.acs.org/10.1021/acschembio.1c00906

The authors declare the following competing financial interest(s): Xuefei Huang is the founder of Iaso Therapeutics Inc., which is dedicated to the development of next generation vaccines using the bacteriophage Qβ platform. Herbert Kavunja is an employee of Iaso. All authors declare no other competing interests.

Department of Chemistry and Institute for Quantitative Health Science and Engineering, Michigan State University, East Lansing, Michigan 48824, United States

Zibin Tan,
Department of Chemistry and Institute for Quantitative Health Science and Engineering, Michigan State University, East Lansing, Michigan 48824, United States

Shuyao Lang,
Department of Chemistry and Institute for Quantitative Health Science and Engineering, Michigan State University, East Lansing, Michigan 48824, United States

Setare Tahmasebi Nick,
Department of Chemistry and Institute for Quantitative Health Science and Engineering, Michigan State University, East Lansing, Michigan 48824, United States

Po-han Lin,
Department of Chemistry and Institute for Quantitative Health Science and Engineering, Michigan State University, East Lansing, Michigan 48824, United States

Zhaojun Yin,
Department of Chemistry, Michigan State University, East Lansing, Michigan 48824, United States

Sherif Ramadan,
Department of Chemistry and Institute for Quantitative Health Science and Engineering, Michigan State University, East Lansing, Michigan 48824, United States

Chemistry Department, Faculty of Science, Benha University, Benha, Qaliobiya 13518, Egypt

Xiangshu Jin,
Department of Chemistry, Michigan State University, East Lansing, Michigan 48824, United States

Xuefei Huang
Department of Chemistry, Institute for Quantitative Health Science and Engineering, and Department of Biomedical Engineering, Michigan State University, East Lansing, Michigan 48824, United States

Abstract

Vaccines are critical tools to treat and prevent diseases. For an effective conjugate vaccine, the carrier is crucial, but few carriers are available for clinical applications. In addition, a drawback of current protein carriers is that high levels of antibodies against the carrier are induced by the conjugate vaccine, which are known to interfere with the immune responses against the target antigen. To overcome these challenges, we obtained the near atomic resolution crystal structure of an emerging protein carrier, i.e., the bacteriophage Qβ virus like particle. On the basis of the detailed structural information, novel mutants of bacteriophage Qβ (mQβ) have been designed, which upon conjugation with tumor associated carbohydrate antigens (TACAs), a class of important tumor antigens, elicited powerful anti-TACA IgG responses and yet produced lower levels of anticarrier antibodies as compared to those from the wild type Qβ-TACA conjugates. In a therapeutic model against an aggressive breast cancer in mice, 100% unimmunized mice

succumbed to tumors in just 12 days even with chemotherapy. In contrast, 80% of mice immunized with the mQβ-TACA conjugate were completely free from tumors. Besides TACAs, to aid in the development of vaccines to protect against COVID-19, the mQβ based conjugate vaccine has been shown to induce high levels of IgG antibodies against peptide antigens from the SARS-CoV-2 virus, demonstrating its generality. Thus, mQβ is a promising next-generation carrier platform for conjugate vaccines, and structure-based rational design is a powerful strategy to develop new vaccine carriers.

Graphical Abstract

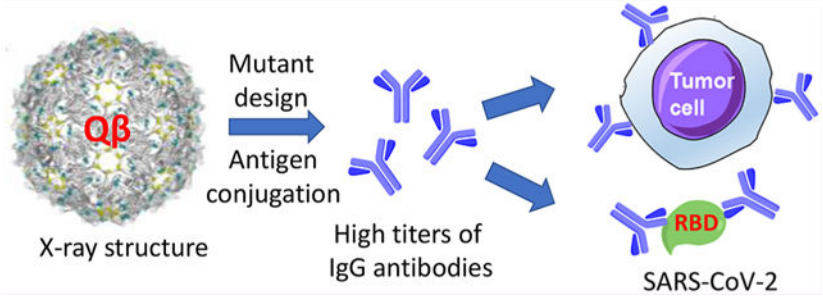

INTRODUCTION

Vaccines have protected humankind from many deadly infections including smallpox, yellow fever, and tetanus, saving millions of lives. However, the rampage of COVID-19 over the world serves as a painful reminder of the constant need for novel vaccines. In addition, the development of effective vaccines for cancer treatment and prevention remains a grand scientific challenge.[1] While deactivated viruses, bacteria, or cancer cells can be utilized as the immunogen, with the increasing demand for vaccine safety, an attractive alternative is the usage of well-defined subunit antigens for vaccine design. However, subunit epitopes typically have reduced immunogenicities.[2] Consequently, immunogenic carrier moieties play an essential role in delivering the antigen and boosting the immune response to fight diseases.[3] As very few carriers have been approved for clinical uses, a powerful new carrier is in high demand.

For conjugate vaccines, an important class of antigens is the tumor associated carbohydrate antigens (TACAs).[4,5] The structures and/or expression levels of carbohydrates on tumor cells can be significantly different from those on normal cells with many TACAs ranked among the top antigens.[6] As TACAs alone cannot generate effective anticancer immune responses, carriers are critical for TACA-based vaccine design. Many carriers have been investigated, such as nanomaterials,[7] liposomes and proteoliposomes,[8] polysaccharides,[9] dendrimers,[10] and immunogenic proteins including keyhole limpet hemocyanin (KLH),[11,12] tetanus toxoid (TT),[13] and cross reactive material-197 (CRM-197).[14,15] KLH,[16] a large glycoprotein, is the most advanced carrier for cancer vaccine studies, as multiple KLH-TACA conjugates have been evaluated in late-stage clinical trials.[11,12] Clinical studies have shown that cancer patients capable of producing high levels of anti-TACA antibodies following KLH-TACA immunization are associated with better prognosis and survival.[17,18] However, for

the full patient cohort, vaccination failed to exhibit statistically significant protection[17,18] highlighting the critical need to improve levels of anti-TACA antibodies produced.

A potential drawback in using an immunogenic protein carrier is that high anticarrier antibody responses can be induced by immunization. As an example, the conjugate of KLH with the GD3 antigen elicited an average anti-GD3 antibody titer of 400 enzyme linked immunosorbent assay (ELISA) units, while that for KLH was 819 200 ELISA units.[19] The high levels of anticarrier antibodies can compete with the production of the antibodies against the target antigen.[20] Furthermore, with the limited range of vaccine carriers, a subject may already have high levels of anticarrier antibodies from prior immunization with other vaccines. The strong anticarrier immunities can suppress anticarbohydrate antibody responses to the new vaccines. These carrier-induced suppression phenomena have been observed in conjugate vaccines.[20,21] When several polysaccharides were conjugated to the same protein carrier, such as TT, after multiple vaccine administrations, the subjects generated significant amounts of anti-TT antibodies. This caused a reduction of the antibody responses to subsequent TT based vaccines as compared with subjects never receiving any prior vaccination with TT as the carrier.[21] Therefore, while carriers are critical to inducing high levels of antibodies against the target antigen, it would be desirable to reduce the antibody responses against the carrier itself to further enhance the levels of anticarbohydrate antibodies that can be induced.

Recently, virus like particles (VLPs) have emerged as a new class of immunogenic carriers for vaccine design.[22,23] Bacteriophage Qβ is a VLP that can elicit high levels of IgG antibodies against multiple types of antigens.[24–27] However, as an immunogenic protein, Qβ can induce strong anti-Qβ antibody responses, which may limit the optimal response against the target antigen. To enhance the ability of Qβ as a vaccine carrier, herein, we report the rational design of new Qβ mutants (mQβ) based on the near atomic resolution crystal structure of Qβ. When conjugated with TACAs, the novel mutants significantly lowered anticarrier antibody responses relative to the corresponding wild type Qβ (wtQβ) conjugate. The mQβ was conjugated with several antigens including the Thomsen-nouveau (Tn) antigen, the GD2 antigen, and peptide epitopes from the SARS-CoV-2 virus. The abilities of these conjugates to induce IgG antibodies were evaluated to establish the power and generality of the mQβ carrier.

RESULTS

Qβ Is a Powerful Carrier to Induce Anti-TACA IgG Antibody Responses.

To test the performance of Qβ as a vaccine carrier, Tn was evaluated as the presentative TACA. Tn is an attractive antigen, as it is detected in 90% of human carcinomas[28] and regarded as one of the more specific human cancer associated structures. A derivative of Tn bearing an *N*-hydroxysuccinimide (NHS) ester (NHS Tn **1**) was synthesized starting from deprotection of the Tn carboxylic acid **2**[29] followed by functionalization with the di-NHS ester **3** of adipic acid (Figure 1a). Tn **1** was then incubated with wtQβ to form the Qβ-Tn conjugate. Mass spectrometry (MS) analysis showed that Qβ-Tn contained an average of 370 Tn per capsid (supplementary Figure S1a). C57BL6 mice were immunized with Qβ-Tn (1.9 μg of Tn per injection) with monophosphoryl lipid A (MPLA) subcutaneously on days

0, 14, and 28 (Figure 1b). Sera were collected from these mice on day 35 after the first immunization. To analyze the levels of anti-Tn antibodies produced, Tn **1** was conjugated with bovine serum albumin (BSA) to form BSA-Tn. ELISA analysis of anti-Tn IgG antibodies was performed using BSA-Tn as the coating antigen (Figure 1c). Qβ-Tn elicited an average anti-Tn IgG antibody titer of 2.4×10^6 ELISA units, which was over 1000 times higher compared to the preimmune sera. The generation of anti-Tn IgG antibodies indicates that the conjugate vaccines were able to activate helper T cells, facilitating the switching of antibody isotypes from IgM to IgG. The immune potentiation effect of Qβ-Tn is specific to Tn as mice receiving Qβ without Tn only gave an average anti-Tn titer around 2000. The high levels of anti-Tn IgG antibodies induced by Qβ-Tn confirm that Qβ is powerful vaccine carrier.

Qβ Can Elicit High Levels of Anti-Qβ Antibodies, and the Heterologous Prime-Boost Protocol Did Not Reduce Anti-Qβ Antibody Responses.

In addition to anti-Tn antibodies, we determined the titers of anti-Qβ IgG antibodies in day 35 sera using Qβ as the coating antigen for ELISA analysis. An average anti-Qβ IgG titer of 5.2×10^6 ELISA units was induced in Qβ-Tn immunized mice, indicating that high levels of anti-Qβ antibodies were generated. As strong anticarrier antibody responses can be detrimental to the generation of antibodies against the target antigen due to carrier induced suppression,[20,21] we hypothesize that the power of the Qβ carrier can be further enhanced if the anti-Qβ antibody responses can be reduced.

One potential approach to reduce the anticarrier responses is the heterologous prime and boost strategy.[30] The Tn conjugate with another VLP, Cowpea Mosaic Virus (CPMV-Tn),[29] was synthesized. Mice were immunized with the Qβ-Tn conjugate on day 0, then CPMV-Tn on day 14, followed by Qβ-Tn on day 28. In this strategy, as epitopes from Qβ and CPMV should be different due to the low sequence homology between the two VLPs, the Tn antigen is the only component common in all injections. Thus, anti-Tn immunity should benefit the most from boost injections. However, from mice immunized with the heterologous prime and boost strategy using Qβ-Tn and CPMV-Tn, anti-Qβ IgG titers in day 35 sera remained at a high level, while the anti-Tn IgG titers were significantly lower compared to when the Qβ-Tn conjugate was used for all three immunizations (data not shown). These results may be because Qβ was more powerful in inducing anti-Tn antibodies than CPMV, which prompted us to focus on engineering Qβ to reduce the anticarrier responses.

Major B Cell Epitopes of Qβ Do Not Reside within a Linear Sequence.

The production of anti-Qβ antibodies originates from the recognition of B cell epitopes on the exterior of the Qβ capsid by Qβ specific B cells. To identify the B cell epitopes, we first performed epitope screening using a peptide library. The Qβ VLP capsid is formed mainly through the self-assembly of 180 copies of a monomeric coat protein containing 132 amino acid residues.[31] We synthesized eight 30 amino acid peptides with sequences overlapping by 15 amino acids covering the full sequence of the Qβ coat protein. These peptides were immobilized into ELISA wells individually, and sera from Qβ immunized mice were added to each well to test the recognition of each peptide by the sera. As shown in supplementary

Figure S2, none of the synthetic peptides showed strong binding to anti-Qβ IgG antibodies in the postimmune sera as compared to the intact capsid. These results suggest that the B cell epitopes of Qβ do not reside within a linear sequence. Rather, they are most likely conformational (i.e., residues are far apart in the primary sequence but close to each other in the tertiary structure).

To identify the epitopes of Qβ, one approach would be to individually mutate all 132 amino acid residues and identify mutations reducing binding to anti-Qβ antibodies. However, this would require the tedious and labor-intensive process of generating and screening a large number of mutants. To guide our carrier design, we looked to the Qβ VLP structure for insights.

The Crystal Structure of Qβ Provides Critical Insights for Guiding Qβ Mutant Design to Reduce Anticarrier Antibody Production.

Compared to carrier proteins that are amorphous such as KLH, an advantage of Qβ is that it has a highly organized structure enabling crystallography studies. While Qβ structure was reported before for the live phage,[31] Qβ VLP has a different surface protein composition. To obtain structural insights, Qβ VLP was crystallized, and its structure was solved by X-ray crystallography at 4.2 Å resolution (PDB code 7TJM), which provided valuable information to guide the selection of the residues of the Qβ VLP to be mutated. We envision that due to the large sizes of B cell receptors (similar to those of antibodies), B cell epitopes of Qβ most likely reside on the external surface of the Qβ capsid and are well exposed to solvents so that they can bind with the bulky B cell receptors on the corresponding Qβ-specific B cells. The relative accessible surface area (RASA) was calculated for each residue in the Qβ VLP crystal structure. As shown in Figure 2a, asparagine 10 (N10), lysine 16 (K16), alanine 38 (A38), threonine 75 (T75), and glutamic acid 103 (E103) are among the most surface-accessible residues on the capsid exterior. In addition, the Qβ structure was analyzed using DiscoTope 2.0,[32] a program for predicting discontinuous B cell epitopes based on the surface accessibility and the spatial neighborhood of the residues. The analysis suggests that residues K16, A38, T75, and E103 reside in areas of high potential B cell epitopes (Figure 2a). As K16 is a major site for derivatization when Qβ is subjected to amide formation reactions,[33] A38, T75, and E103 were selected for mutation to lysine (K) as these residues face the exterior of the capsid with high SASA or B-cell propensity scores (Figure 2). Lysine is chosen as the mutation target, since it can be an additional site for TACA functionalization. In addition to the B cell epitope change from the mutation, the TACA conjugated at the newly introduced lysine could further shield the nearby B-cell epitope.

Another factor for the mutant design came from a serendipitous discovery. When a Qβ-carbohydrate conjugate was treated with the di-NHS ester of adipic acid **3**, which could cross-link monomer coat protein subunits in a Qβ VLP, significantly higher anticarbohydrate antibody responses were induced by the derivatized Qβ. This was possibly due to the enhanced capsid stability resulting from cross-linking of Qβ subunits. As it was difficult to control the location of cross-linking with the bifunctional linker **3**, we hypothesize that cysteines can be introduced near the interface between subunits of Qβ VLP, which can potentially form disulfide bonds to cross-link the subunits and enhance anti-TACA antibody

responses. However, mutations of residues directly involved in intersubunit interactions should be avoided to prevent obstructions of VLP assembly. Analysis of the crystal structure of Qβ VLP revealed that alanine 40 (A40) and aspartic acid 102 (D102) on adjacent coat protein monomers are in close proximity and a disulfide bond between these two residues would further strengthen intersubunit cross-linking of the capsid (Figure 3). Thus, A40 and D102 were selected as sites for mutation to cysteines for potential disulfide bond formation.

The designed mutant Qβ (mQβ) VLPs were cloned and expressed in *E. coli*. Although E103 K failed to assemble, the A38K, T75K, A40C/D102C, A40S/D102S (a chemically equivalent mutant to A40C/D102C but unable to form a disulfide bond between residues 40 and 102), and A38K/A40C/D102C mutants formed nanoparticles with similar expression yields as that for wtQβ (~30 mg/L). The sizes of the mutants were also similar to that of wtQβ based on transmission electron microscopy (TEM) analysis (supplementary Figure S3). The characteristic properties of all mQβ capsids are summarized in supplementary Table S1.

mQβ Capsids Containing A40C/D102C Mutations Have an Additional Disulfide Bond Formed between C40 and C102 and Have Higher Thermal Stabilities.

To confirm that A40C/D102C formed a disulfide bond, nonreducing and reducing SDS-PAGE gel electrophoresis results of mQβs were compared (supplementary Figure S4). While most capsids broke down to their monomer on a reducing SDS-PAGE gel (supplementary Figure 4Sb), all mQβs containing A40C/D102C mutations showed high molecular weight protein bands in the stacking gel of nonreducing conditions (supplementary Figure S4a). This is presumably due to the multimerization of the subunits. The chemically equivalent mutants lacking the disulfide bond, A40S/D102S, showed similar gel patterns as wtQβ VLP. These results verified the formation of additional disulfide bonds in mutants containing A40C/D102C.

The effect of A40C/D102C mutations on capsid stability was evaluated next through melting temperature measurement (supplementary Figure S5). The wtQβ had a melting temperature of 79 °C when it started to denature as indicated by the changes in its UV–vis absorbance. The mQβ A40C/D102C capsid had a higher stability as demonstrated by its increased melting temperature of 84 °C. The melting temperature of the chemically similar mutant, A40S/D102S, dropped to 76 °C, supporting the importance of the disulfide for stabilizing the capsid.[34] Similar stabilizing effects were observed when mQβ A38K/A40C/D102C (melting *T*: 80 °C) was compared to mQβ A38K (melting *T*: 74 °C). The higher stability of the capsid can be beneficial as the vaccine constructs can potentially provide longer stimulation to the immune system resulting in stronger immune responses.

The New mQβs Can Significantly Enhance Levels of Antibodies against the Tn Antigen, while Reducing Anticarrier Antibody Responses.

To assess the potency of mQβ in inducing immunity against TACA and the carrier itself, the Tn antigen **1** was conjugated with mQβ under identical reaction conditions to those of the wtQβ (Figure 1a). The numbers of Tn on A38K, T75K, A40C/D102C, and A38K/A40C/D102C were controlled to be at similar levels to those of the wtQβ construct by adjusting

the amount of Tn **1** added to the reaction. Mice (n = 5) were vaccinated with wtQβ-Tn and mQβ-Tn conjugates (all at 1.9 μg of Tn with MPLA as the adjuvant) following the aforementioned protocol of three biweekly injections (Figure 1b). The sera from immunized mice were collected on day 35 and analyzed for the levels of anti-Tn and anticarrier IgG antibodies.

For mQβ-Tn conjugates, while the T75K mutant led to comparable anti-Tn IgG titers as the wtQβ-Tn conjugate, A38K, A40C/D102C, and A38K/A40C/D102C produced significantly higher levels of anti-Tn IgG responses (Figure 4a). The mean anti-Tn IgG titers generated by mQβ(A38K/A40C/D102C)-Tn were close to 10 times those induced by wtQβ-Tn, reaching 1.8×10^7 ELISA units. To the best of our knowledge, this is the highest anti-Tn titer reported to date. Antibody subtype analysis showed all major IgG subtypes were produced indicating balanced T-cell-dependent immune responses (supplementary Figure S6).

We tested the impacts of mutations on levels of anticarrier antibodies subsequently. The levels of IgG antibodies elicited by wtQβ, mQβ(A38K), mQβ(A40C/D102C), and mQβ-(A38K/A40C/D102C) recognizing wtQβ were measured first against wtQβ immobilized in ELISA wells. As shown in Figure 4b, all mQβ conjugates elicited much lower levels of anti-wtQβ antibodies compared to the wtQβ conjugate with the anti-wtQβ IgG antibody titers induced by mQβ(A38K/A40C/D102C) at 25% of that by the wtQβ. It is possible that mutations can create new B cell epitopes in mQβ. We next analyzed antibody responses against the mQβ. All mQβ generated fewer IgG antibodies against the mQβ(A38K/A40C/D102C) as compared to the level of anti-wtQβ antibodies elicited by wtQβ (Figure 4c). Correlation with anti-Tn antibody responses from Tn conjugates of A38K, A40C/D102C, and A38K/A40C/D102C exhibited an interesting reverse trend of anticarrier vs anti-Tn antibodies (supplementary Figure S7a,b) with the vaccine construct producing lower anticarrier antibody responses eliciting higher levels of anti-Tn IgG. mQβ(A38K/A40C/D102C) was selected as the lead carrier for further evaluation.

With the high levels of antibodies against Tn generated in postimmune sera, it is important to determine the abilities of the antibodies to recognize tumor cells expressing Tn, such as TA3Ha, a mouse breast cancer cell line. Flow cytometry analysis showed that the IgG antibodies elicited by mQβ-(A38K/A40C/D102C)-Tn exhibited significantly stronger binding to TA3Ha cells compared to tumor cell binding by sera from wtQβ-Tn immunized mice (Figure 5). These results suggest the antibodies induced by mQβ-Tn can recognize Tn in its native environment, i.e., on the surface of tumor cells, which bodes well as anticancer vaccines.

mQβ Is a Superior TACA Carrier Compared to Common Benchmark Protein Carriers.

To benchmark the mQβ carrier, head-to-head comparison studies were performed between mQβ and the three most common benchmark protein carriers, i.e., KLH, TT, and CRM-197. Tn **1** was conjugated with KLH, TT, and CRM-197, respectively, through the same method as mQβ-Tn using NHS Tn **1** (Figure 1a). Mice were immunized with KLH-Tn, TT-Tn, and CRM-197-Tn conjugates with the same dose of Tn (1.9 μg of Tn) and MPLA adjuvant three times biweekly. On day 35, sera were collected from immunized mice, and the anti-Tn IgG antibody titers were measured by ELISA against BSA-Tn. KLH-Tn, TT-Tn, and

CRM-197-Tn conjugates induced average anti-Tn IgG titers of 3.2×10^6, 2.4×10^6, and 6.6×10^6 ELISA units, respectively, which were significantly lower than those from mQβ-Tn immunized mice (average anti-Tn titer of 18×10^6 ELISA units; supplementary Figure S7c). Thus, mQβ is a superior vaccine carrier compared to the commonly utilized gold standard carriers in delivering the Tn antigen.

mQβ Carrier Significantly Enhanced Antibody Responses against Another TACA, the GD2 Antigen.

To test the generality of mQβ, besides the Tn antigen, we investigated its utility in targeting another TACA, GD2, which is overexpressed on cancers including lymphoma, osteosarcoma, and neuroblastoma.[35] A derivative of the GD2 antigen NHAcGD2 **3**[36] was conjugated with wtQβ and mQβ(A38K/A40C/D102C) (Figure 6a). Mice were immunized with these two conjugates respectively three times following the same biweekly schedule as in the Tn vaccine study. Sera from immunized mice 35 days after immunization were collected and analyzed.

The mQβ conjugate induced superior immune responses against GD2 as compared to its wtQβ counterpart. ELISA analysis showed that while wtQβ-NHAcGD2 elicited an average anti-NHAcGD2 IgG titer of 7.5×10^5 ELISA units, immunization with the corresponding mQβ(A38K/A40C/D102C)-NHAcGD2 conjugate led to significantly higher IgG titers reaching 1.1×10^6 ELISA units (Figure 6b). Furthermore, the abilities of the antibodies to kill GD2 expressing EL4 lymphoma cells were analyzed using a complement mediated cytotoxicity assay. Sera from mQβ-(A38K/A40C/D102C)-NHAcGD2 immunized mice exhibited significantly higher cytotoxicity against GD2 expressing EL4 lymphoma cells compared to those from mice immunized with wtQβ-NHAcGD2 (Figure 6c).

mQβ Conjugate Can Induce High Levels of Antibodies against SARS-CoV-2 Associated Peptide Antigens.

Besides carbohydrates, peptides are another common class of antigens for conjugate vaccines. To test the applicability of mQβ carrier in peptide-based vaccines, we selected peptide epitopes from the SARS-CoV-2 virus. While the availability of several vaccines has fundamentally changed the landscape of fighting COVID-19, there are limitations of current vaccines including rapid waning of induced immunity and reduced efficacy against variants of the virus.[37] Thus, continual development of anti-SARS-CoV-2 vaccines is needed.

Two potential B cell peptide epitopes (peptides **4** and **5**) from the receptor binding domain (RBD) of the SARS-CoV-2 virus were designed, which contained amino acid residues 407–428 and 473–491 of the spike protein (Figure 7a).[38] The RBD is critical for the virus to bind and infect human epithelial cells, and anti-RBD antibodies can block the viral entry into cells protecting the host from infection.[39,40] Several RBD-based conjugate or nanoparticle vaccines have been investigated.[41–44] In our work, to test the scope of conjugation chemistry on mQβ, sulfhydryl chemistry was explored by adding a cysteine residue to the *N*-terminus of aa 407–428 (peptide **4**). mQβ was treated with the acrylic ketone linker **6**,[45] which was followed by incubation with the peptide **4** (Figure 7b). On average, 277 copies of the peptide could be attached per capsid. Peptide **5** was conjugated to mQβ by amide bonds

through a bifunctional activated ester linker **7**[46] (Figure 7c). Mice were immunized with the mQβ-RBD peptides **4** and **5** three times biweekly. Analysis of day 35 sera of the immunized mice showed that average titers of 2.3×10^6 and 1.1×10^6 ELISA units of IgG antibodies were produced in immunized mice against the peptide antigens (Figure 7d). Furthermore, the postimmune sera also recognized the full RBD glycoprotein well with average IgG titers of 1.8×10^5 and 5.2×10^4 ELISA units against the RBD (Figure 7e). Thus, the mQβ-RBD peptide conjugates are promising leads for new anti-SARS-CoV-2 vaccines. The factors potentially impacting anti-RBD antibody responses to **4** and **5** include the nature of the peptide epitopes, the conjugation methods used, and the level of antigen loading. Further studies are needed to dissect the effects of these parameters.

Immunization with mQβ-Tn Conjugate Provided Superior Protection to Mice in an Aggressive Breast Cancer Model.

Beyond analysis of antibody levels and functions *in vitro*, a critical test for the efficacy of a vaccine is *in vivo* protection. With the ability of mQβ-Tn conjugate to elicit higher levels of anti-Tn IgG antibodies established, we moved onto tumor protection by mQβ-Tn *in vivo* against TA3Ha murine mammary adenocarcinoma. TA3Ha is a highly aggressive tumor, as 10 000 TA3Ha cells injected intraperitoneally were sufficient to kill all mice within 11 days due to tumor growth (Figure 8a), thus presenting a challenging model for tumor protection studies.

To mimic clinical conditions for cancer treatment, we evaluated the vaccine efficacy in a therapeutic setting. Mice were injected with TA3HA cells first to establish tumors, which were then vaccinated with the Qβ-Tn construct. To enhance the therapeutic efficacy, Qβ-Tn immunotherapy was combined with cyclophosphamide (CP) chemotherapy, a common drug used for breast cancer treatment in human patients. While CP does not directly kill tumor cells at the dose administered[47] and its anticancer mechanisms are complex,[48] CP can potentially reduce the immunosuppression imposed by myeloid-derived suppressor cells and activate the effector cells such as natural killer cells to enhance vaccine efficacy.[49]

Following the inoculation of 10 000 TA3Ha cells to mice, on day 1, mice were treated with CP. Subsequently, they received wtQβ-Tn or mQβ(A38K/A40C/D102C)-Tn on days 1, 4, and 8, respectively, or PBS buffer as the mock control. The survival of all four groups of mice was monitored over time. Administration of CP only bestowed little survival advantage to mice as all mice died by day 12 post tumor inoculation (Figure 8a). wtQβ-Tn immunization provided protection with 20% of the mice surviving the tumor. In comparison, 80% of the mice vaccinated with mQβ(A38K/A40C/D102C)-Tn were tumor free on day 25 post tumor challenge. Furthermore, mice alive in the mQβ(A38K/A40C/D102C)-Tn group were rechallenged with 10 000 TA3Ha cells (Figure 8b). Without any further vaccination or treatment, all mice survived the second tumor challenge with no tumor recurrence, suggesting effective anticancer immunity was induced without the need for further vaccination.

DISCUSSION

Multiple clinical studies have shown that the prognosis of cancer patients can be correlated with the levels of anti-TACA antibodies.[17,18] Thus, vaccines capable of eliciting high titers of anti-TACA antibodies are highly attractive for tumor protection. The development of anticancer vaccines and the improvement of immune responses are multifaceted processes, which include antigen engineering, adjuvants, and carrier structures. Carrier molecules are critical to delivering the weakly immunogenic antigens such as TACA to the immune system and to boost the anti-TACA immunity.

VLPs as represented by Qβ are a class of powerful carriers for conjugate vaccines. Compared to amorphous carriers such as KLH, VLPs have well-defined three-dimensional structures for high density organized display of antigens, which is important for potent antibody generation.[50] Furthermore, VLPs such as Qβ can encapsulate RNA inside the particles, which can activate Toll like receptor 7 and help enhance the immunogenicity of the conjugate.[51]

A potential drawback in using a highly immunogenic protein as the vaccine carrier is that strong anticarrier antibody responses can be induced. Mice with high titers of anti-Qβ IgG antibodies have been shown to produce much fewer antipeptide antibodies upon immunization with a Qβ-peptide conjugate.[52] There are multiple possible reasons for the suppression of antibodies against the conjugated target antigen, such as TACAs, due to anti-Qβ antibodies. (1) As anti-Qβ antibodies are generated earlier than those against the TACAs,[53] during boost injection, the existing anti-Qβ antibodies can bind with the vaccine construct, sterically hindering the recognition of glycan epitopes by glycan specific B cells. (2) Anti-Qβ antibodies can bind with the vaccine construct, sequestering the construct and reducing the availability of construct to interact with glycan specific B cells. (3) Anti-Qβ B-cells can compete with anti-TACA B-cells for limited helper T-cell stimulation. Thus, an ideal carrier would be a molecule that induces a low antibody response to itself but a high antibody response to the hapten.[54,55] Removing B cell epitopes from Qβ may enable the immune system to focus more on the desired TACA, enhancing antiglycan responses.

Experimental identification of B-cell epitopes can be challenging, especially when the epitopes are mainly conformational, not residing within a linear sequence as in the case of Qβ. One major advantage of Qβ is with its well-ordered structure, the crystal structure of Qβ VLP has been obtained in high resolution. This provided extremely valuable guidance for mutant design to reduce anticarrier antibody responses. From structure-based analysis, residues with high solvent exposure and potential to be B cell epitopes have been identified, which serve as targets for mutations to disrupt the inherent B cell epitopes. In addition, sites have been identified for the introduction of cross-subunit disulfide bonds and to avoid the disruption of capsid assembly. From multiple mutants developed, the triple mutant mQβ(A38K/A40C/D102C) has been identified as the lead construct.

Multiple factors in combination may contribute to higher titers of anti-Tn IgG antibodies and lower anticapsid antibodies induced by the triple mutant A38K/A40C/D102C. A38K mutation can remove the potential B cell epitopes of wtQβ as A38 resides in a region

predicted to be recognized by B cells. The newly introduced lysine can be derivatized with Tn further shielding the nearby B cell epitopes of the coat protein. Another potential factor is the enhanced thermal stability of mQβs containing A40C and D102C mutations. As new disulfide bonds are introduced, these mutants are more stable than those without the mutations. The higher stability of the vaccine construct may increase the half-life of the vaccine *in vivo*, prolonging the stimulation of the immune system.

CONCLUSIONS

Carriers are crucial for the development of effective conjugate vaccines to powerfully boost antibody responses against weakly immunogenic subunit antigens. With the paucity of validated carriers for clinical studies, new carrier moieties are urgently needed. Bacteriophage Qβ VLP is a powerful carrier for conjugate vaccines. To further enhance the carrier ability of Qβ, the X-ray crystal structure of Qβ VLP was obtained. By examining the near atomic resolution structure of Qβ, strategic sites were identified for mutant design to remove/camouflage the endogenous B cell epitopes of Qβ and to enhance the capsid's thermal stability. Among the various mutants explored, the triple mutant mQβ(A38K/A40C/D102C) was identified to be the lead construct. Conjugates of mQβ with the Tn antigen were able to induce superior anti-Tn antibodies compared to the corresponding wtQβ conjugate, as well as multiple common benchmark protein carriers. In an aggressive breast cancer model, while all nonimmunized mice succumbed to the tumor in just 11 days, the mQβ-Tn conjugate significantly enhanced the survival rate of the mice to 80% from 20% bestowed by the wtQβ-Tn construct. In addition, mQβ powerfully boosted antibody responses against another TACA, NHAcGD2. Besides carbohydrate antigens, peptide antigens from SARS-CoV-2 were efficiently conjugated with mQβ, including through the sulfhydryl reaction with an acrylic ketone linker, broadening the scope of antigens that can be targeted. The mQβ-SARS-CoV-2 peptide conjugates induced high levels of IgG antibodies not only against the peptide but also against the full RBD glycoprotein, demonstrating the generality of the carrier. The powerful antibody potentiation abilities coupled with the reduced anticarrier responses associated with mQβ renders it a highly attractive platform for next generation conjugate vaccine development.

METHODS

Qβ Viral Capsid Protein Expression and Purification.

A single colony of BL21(DE3)pLysS *E. coli* with the mutated plasmid was selected to be inoculated into a starter culture of 50 mL of SOC containing 20 μg/mL Kanamycin. The starter culture was grown overnight in a shaker incubator at 37 °C with a shaking speed of 230 rpm. After overnight, the resulting cloudy culture was then transferred into 1 L of culture medium with the antibiotic selection. The culture was continued under the same conditions until the OD_{600} value was between 0.7 and 1.0. Isopropyl β-D-1-thiogalactopyranoside (IPTG; 1 mL of 1M) was then added into the culture to induce protein expression (final concentration = 1 mM). The culture was continued 4–5 h. The bacteria were then pelleted at 6000 rpm for 30 min. The culture medium was discarded. The pellets were resuspended in 0.1 M PBS pH 7 (10 mL). The bacteria in the suspension were then

lysed with a probe sonicator in an ice bath. The sonication generator was set at a power of 30% for 10 min with interval of 5 s pulses and 5 s stops. The lysis was centrifuged at 14 000 rpm for 20 min. PEG 8000 was added to the supernatant containing the capsid protein to a final concentration of 10% (w/v) and put on a nutating mixer at 4 °C overnight to allow complete protein precipitation. The precipitate was pelleted down at 14 000 rpm for 20 min. The pellet was resuspended in 0.1 M PBS at pH = 7. The resuspended solution was 1:1 (v/v) mixed with 1:1 (v/v) chloroform/n-butanol until the mixture turned into a colloid. The colloidal mixture was centrifuged at 7000 rpm for 1 h to separate the layers. The top (aqueous) layer was collected. Viral capsid protein in the collected aqueous layer was concentrated down through Millipore 100k MWCO and further purified by sucrose density gradients 10–40% (w/v). The linear (continuous) sucrose gradients were prepared following a freezing–thawing method.[56] The loaded sucrose gradients were centrifuged with the SW32 swing bucket rotor at 28 000 rpm for 5 h. The viral capsid band was visualized by LED light shining through the top of the tube. The bright blue band from scattering light was collected as fractions of 1 mL. The collected fraction was analyzed for purity of the capsid by size-exclusion chromatography using a Superose 6 column 10/300 (void volume = 9 mL). The fraction that showed a single peak at elution around 11–15 mL was determined as the VLP mQβ with RNA encapsulated. The remaining sucrose in the collected fraction was removed by filtration through a Millipore 100k MWCO centrifugal filter tube and washed thoroughly with a PBS buffer. The total protein concentration in the final solution was quantified with a Pierce BCA Protein Assay Kit with bovine serum albumin as the standard. The purified VLP was characterized by size-exclusion chromatography, dynamic light scattering (DLS), and TEM for particles' size, homogeneity, shape, and purity. The change of the amino acid(s) as a result of the mutation was determined by the molecular weight difference compared with wide-type Qβ. The molecular weight of the protein was determined by LCMS QTOF ESI mass spectroscopy, and the multiple charge mass spectra were transformed to single charge uing the maximum entropy deconvolution algorithm (MaxEnt 1).

Immunization Studies.

Pathogen-free C57BL/6 female mice aged 6–10 weeks were obtained from the Jackson Laboratory and maintained in the University Laboratory Animal Resources facility of Michigan State University. All animal care procedures and experimental protocols have been approved by the Institutional Animal Care and Use Committee (IACUC) of Michigan State University. Groups of five mice were injected subcutaneously under the scruff on day 0 with 0.1 mL of various Qβ constructs, or protein-Tn conjugate mixed together with MPLA (20 μg) as the adjuvant, and boosters were given subcutaneously under the scruff on days 14 and 28 with 0.1 mL of various Qβ constructs with MPLA (20 μg) as the adjuvant. All Tn vaccine constructs administered have the same amounts of Tn antigen (1.9 μg). Serum samples were collected on days 0 (before immunization) and 35. The final bleeding was done by cardiac bleed.

Antitumor Immunotherapy.

TA3Ha cells (10 000 cells) were intraperitoneally injected into eight-week old female C57BL6 mice on day 0. Mice were injected with PBS buffer or cyclophosphamide (50

mg/kg) intraperitoneally on day 1 (n = 10 for each group). wtQβ-Tn or mQβ(A38K/A40C/D102C)-Tn with MPLA (20 μg) was administrated intraperitoneally on days 1, 4, and 8, respectively, while only PBS buffer was injected for the PBS group. Survival of mice was monitored for 25 days. Mice free of tumors in the mQβ(A38K/A40C/D102C)-Tn group were injected with 10 000 TA3Ha cells intraperitoneally, and the survival of mice was monitored for another 25 days. Statistical analysis of survival was performed with GraphPad Prism using the log-rank test.

Supplementary Material

Refer to Web version on PubMed Central for supplementary material.

ACKNOWLEDGMENTS

We are grateful to the National Institutes of Health (R01CA225105 and R01AI146210) and Michigan State University Foundation for financial support of our work.

REFERENCES

(1). Igarashi Y; Sasada T Cancer Vaccines: Toward the Next Breakthrough in Cancer Immunotherapy. J. Immunol. Res 2020, 2020, 5825401. [PubMed: 33282961]

(2). Vartak A; Sucheck SJ Recent Advances in Subunit Vaccine Carriers. Vaccines 2016, 4, 12 and references cited therein..

(3). Pichichero ME Protein carriers of conjugate vaccines: characteristics, development, and clinical trials. Hum. Vaccin. Immunother 2013, 9, 2505–2523. [PubMed: 23955057]

(4). Guo ZW; Wang QL Recent development in carbohydrate-based cancer vaccines. Curr. Opin. Chem. Biol 2009, 13, 608–617. [PubMed: 19766052]

(5). Yin Z; Huang X Recent development in carbohydrate based anticancer vaccines. J. Carbohydr. Chem 2012, 31, 143–186. and references cited therein. [PubMed: 22468019]

(6). Cheever M; Allison J; Ferris A; Finn O; Hastings B; Hecht T; Mellman I; Prindiville S; Viner J; Weiner L; et al. The prioritization of cancer antigens: a National Cancer Institute pilot project for the acceleration of translational research. Clin. Cancer Res 2009, 15, 5323–5337. [PubMed: 19723653]

(7). Trabbic KR, Kleski KA, Barchi JJ (2021) A Stable Nano-Vaccine for the Targeted Delivery of Tumor-Associated Glycopeptide Antigens. bioRxiv, 2021.2004.2027.438445.

(8). Hossain MK; Vartak A; Sucheck SJ; Wall KA Liposomal Fc Domain Conjugated to a Cancer Vaccine Enhances Both Humoral and Cellular Immunity. ACS Omega 2019, 4, 5204–5208. [PubMed: 30949616]

(9). Ghosh S; Trabbic KR; Shi M; Nishat S; Eradi P; Kleski KA; Andreana PR Chemical synthesis and immunological evaluation of entirely carbohydrate conjugate Globo H-PS A1. Chem. Sci 2020, 11, 13052–13059. [PubMed: 34123241]

(10). Heegaard PMH; Boas U; Sorensen NS Dendrimers for vaccine and immunostimulatory uses. A review. Bioconjuate Chem. 2010, 21, 405–418.

(11). Cheung IY; Cheung NV; Modak S; Mauguen A; Feng Y; Basu E; Roberts SS; Ragupathi G; Kushner BH Survival Impact of Anti-GD2 Antibody Response in a Phase II Ganglioside Vaccine Trial Among Patients With High-Risk Neuroblastoma With Prior Disease Progression. J. Clin. Oncol 2021, 39, 215–226. [PubMed: 33326254]

(12). Huang C-S; Yu AL; Tseng L-M; Chow LWC; Hou M-F; Hurvitz SA; Schwab RB; L Murray J; Chang H-K; Chang H-T; et al. Globo H-KLH vaccine adagloxad simolenin (OBI-822)/OBI-821 in patients with metastatic breast cancer: phase II randomized, placebo-controlled study. J. Immunother. Cancer 2020, 8, e000342. [PubMed: 32718986]

(13). Cai H; Sun ZY; Chen MS; Zhao YF; Kunz H; Li YM Synthetic multivalent glycopeptide-lipopeptide antitumor vaccines: impact of the cluster effect on the killing of tumor cells. Angew. Chem., Int. Ed 2014, 53, 1699–1703.

(14). Zhai C; Zheng X-J; Song C; Ye X-S Synthesis and immunological evaluation of N-acyl modified Globo H derivatives as anticancer vaccine candidates. RSC Med. Chem 2021, 12, 1239–1243. [PubMed: 34355188]

(15). Kleski KA; Andreana PR Developments in CRM197 Glycoconjugates for Anticancer Vaccines. Am. J. Biomed. Sci. Res 2019, 6, 212.

(16). Harris JR; Markl* J Keyhole limpet hemocyanin (KLH): a biomedical review. Micron 1999, 30, 597–623. [PubMed: 10544506]

(17). Huang C-S; Yu AL; Tseng L-M; Chow LWC; Hou M-F; Hurvitz SA; Schwab RB; Wong C-H; Murray JL; Chang H-K; Chang H-T; Chen S-C; Kim S-B; Shue Y-K; Rugo HS; et al. Randomized phase II/III trial of active immunotherapy with OPT822/OPT821 in patients with metastatic breast cancer. J. Clin. Oncol 2016, 34, 1003.

(18). Oei ALM; Moreno M; Verheijen RHM; Sweep FCGJ; Thomas CMG; Massuger LFAG; Von Mensdorff-Pouilly S Induction of IgG antibodies to MUC1 and survival in patients with epithelial ovarian cancer. Int. J. Cancer 2008, 123, 1848–1853. [PubMed: 18661524]

(19). Deng K; Adams MM; Damani P; Livingston PO; Ragupathi G; Gin DY Synthesis of QS-21-Xylose: Establishment of the Immunopotentiating Activity of Synthetic QS-21 Adjuvant with a Melanoma Vaccine. Angew. Chem., Int. Ed 2008, 47, 6395–6398.

(20). Fattom A; Cho YH; Chu C; Fuller S; Fries L; Naso R Epitopic overload at the site of injection may result in suppression of the immune response to combined capsular polysaccharide conjugate vaccines. Vaccine 1999, 17, 126–133. [PubMed: 9987146]

(21). Dagan R; Eskola J; Leclerc C; Leroy O Reduced Response to Multiple Vaccines Sharing Common Protein Epitopes That Are Administered Simultaneously to Infants. Infect. Immun 1998, 66, 2093–2098. [PubMed: 9573094]

(22). Chung YH; Cai H; Steinmetz NF Viral nanoparticles for drug delivery, imaging, immunotherapy, and theranostic applications. Adv. Drug Delivery Rev 2020, 156, 214–235.

(23). Bachmann MF; Jennings GT Vaccine delivery: a matter of size, geometry, kinetics and molecular patterns. Nat. Rev. Immunol 2010, 10, 787–796. [PubMed: 20948547]

(24). Dhara D; Baliban SM; Huo C-X; Rashidijahanabad Z; Sears KT; Nick ST; Misra AK; Tennant SM; Huang X Syntheses of Salmonella Paratyphi A Associated Oligosaccharide Antigens and Development towards Anti-Paratyphoid Fever Vaccines. Chem.—Eur. J 2020, 26, 15953–15968. [PubMed: 32578281]

(25). Wang P; Huo C-X; Lang S; Caution K; Nick ST; Dubey P; Deora R; Huang X Chemical Synthesis and Immunological Evaluation of a Pentasaccharide Bearing Multiple Rare Sugars as a Potential Anti-pertussis Vaccine. Angew. Chem., Int. Ed 2020, 59, 6451–6458.

(26). Wu X; Yin Z; McKay C; Pett C; Yu J; Schorlemer M; Gohl T; Sungsuwan S; Ramadan S; Baniel C; et al. Protective epitope discovery and design of MUC1-based vaccine for effective tumor protections in immunotolerant mice. J. Am. Chem. Soc 2018, 140, 16596–16609. [PubMed: 30398345]

(27). Polonskaya Z; Deng S; Sarkar A; Kain L; Comellas-Aragones M; McKay CS; Kaczanowska K; Holt M; McBride R; Palomo V; et al. T cells control the generation of nanomolar-affinity anti-glycan antibodies. J. Clin. Invest 2017, 127, 1491–1504. [PubMed: 28287405]

(28). Springer GF T and Tn, General Carcinoma Autoantigens. Science 1984, 224, 1198–1206. [PubMed: 6729450]

(29). Miermont A; Barnhill H; Strable E; Lu X; Wall KA; Wang Q; Finn MG; Huang X Cowpea mosaic virus capsid: A promising carrier for the development of carbohydrate based antitumor vaccines. Chem.—Eur. J 2008, 14, 4939–4947. [PubMed: 18431733]

(30). Lu S Heterologous prime-boost vaccination. Curr. Opin. Immunol 2009, 21, 346–351. [PubMed: 19500964]

(31). Golmohammadi R; Fridborg K; Bundule M; Valegard K; Liljas L The crystal structure of bacteriophage Qβ at 3.5Å resolution. Structure 1996, 4, 543–554. [PubMed: 8736553]

(32). Kringelum JV; Lundegaard C; Lund O; Nielsen M Reliable B cell epitope predictions: impacts of method development and improved benchmarking. PLoS Comput. Biol 2012, 8, e1002829. [PubMed: 23300419]

(33). https://docplayer.net/30915020-Analytical-control-strategy-for-a-vlp-peptide-conjugate-vaccine.html

(34). Fiedler JD; Higginson C; Hovlid ML; Kislukhin AA; Castillejos A; Manzenrieder F; Campbell MG; Voss NR; Potter CS; Carragher B; et al. Engineered mutations change the structure and stability of a virus-like particle. Biomacromolecules 2012, 13, 2339–2348. [PubMed: 22830650]

(35). Cavdarli S; Dewald JH; Yamakawa N; Guérardel Y; Terme M; Le Doussal J-M; Delannoy P; Groux-Degroote S Identification of 9-O-acetyl-N-acetylneuraminic acid (Neu5,9Ac2) as main O-acetylated sialic acid species of GD2 in breast cancer cells. Glycoconj. J 2019, 36, 79–90 and references cited therein.. [PubMed: 30612272]

(36). Wu X; Ye J; DeLaitsch AT; Rashidijahanabad Z; Lang S; Kakeshpour T; Zhao Y; Ramadan S; Saavedra PV; Yuzbasiyan-Gurkan V; Kavunja H; Cao H; Gildersleeve JC; Huang X; et al. Chemoenzymatic Synthesis of 9NHAc-GD2 Antigen to Overcome the Hydrolytic Instability of O-Acetylated-GD2 for Potential Anticancer Conjugate Vaccines. Angew. Chem., Int. Ed 2021, 60, 24179–24188.

(37). Planas D; Veyer D; Baidaliuk A; Staropoli I; Guivel-Benhassine F; Rajah MM; Planchais C; Porrot F; Robillard N; Puech J; et al. Reduced sensitivity of SARS-CoV-2 variant Delta to antibody neutralization. Nature 2021, 596, 276–280. [PubMed: 34237773]

(38). Wu F; Zhao S; Yu B; Chen Y-M; Wang W; Song Z-G; Hu Y; Tao Z-W; Tian J-H; Pei Y-Y; et al. A new coronavirus associated with human respiratory disease in China. Nature 2020, 579, 265–269. [PubMed: 32015508]

(39). Wu Y; Wang F; Shen C; Peng W; Li D; Zhao C; Li Z; Li S; Bi Y; Yang Y; et al. A noncompeting pair of human neutralizing antibodies block COVID-19 virus binding to its receptor ACE2. Science 2020, 368, 1274–1278. [PubMed: 32404477]

(40). Liu C; Zhou Q; Li Y; Garner LV; Watkins SP; Carter LJ; Smoot J; Gregg AC; Daniels AD; Jervey S; et al. Research and development on therapeutic agents and vaccines for COVID-19 and related human coronavirus diseases. ACS Cent. Sci 2020, 6, 315–331. [PubMed: 32226821]

(41). Zhao Q; Gao Y; Xiao M; Huang X; Wu X Synthesis and immunological evaluation of synthetic peptide based anti-SARS-CoV-2 vaccine candidates. Chem. Commun 2021, 57, 1474–1477.

(42). Li M; Jin R; Peng Y; Wang C; Ren W; Lv F; Gong S; Fang F; Wang Q; Li J; et al. (2020) Generation of antibodies against COVID-19 virus for development of diagnostic tools. medRxiv, 2020.2002.2020.20025999.

(43). Ma X; Zou F; Yu F; Li R; Yuan Y; Zhang Y; Zhang X; Deng J; Chen T; Song Z; Qiao Y; Zhan Y; Liu J; Zhang J; Zhang X; Peng Z; Li Y; Lin Y; Liang L; Wang G; Chen Y; Chen Q; Pan T; He X; Zhang H Nanoparticle Vaccines Based on the Receptor Binding Domain (RBD) and Heptad Repeat (HR) of SARS-CoV-2 Elicit Robust Protective Immune Responses. Immunity 2020, 53, 1315. [PubMed: 33275896]

(44). Valdes-Balbin Y; Santana-Mederos D; Quintero L; Fernández S; Rodriguez L; Sanchez Ramirez B; Perez-Nicado R; Acosta C; Méndez Y; Ricardo MG; et al. SARS-CoV-2 RBD-Tetanus Toxoid Conjugate Vaccine Induces a Strong Neutralizing Immunity in Preclinical Studies. ACS Chem. Biol 2021, 16, 1223–1233. [PubMed: 34219448]

(45). Bernardim B; Cal PMSD; Matos MJ; Oliveira BL; Martinez-Saez N; Albuquerque IS; Perkins E; Corzana F; Burtoloso ACB; Jimenez-Oses G; Bernardes GJL; et al. Stoichiometric and irreversible cysteine-selective protein modification using carbonylacrylic reagents. Nat. Commun 2016, 7, 13128. [PubMed: 27782215]

(46). Wu X; Ling C-C; Bundle DR A New Homobifunctional *p*-Nitro Phenyl Ester Coupling Reagent for the Preparation of Neoglycoproteins. Org. Lett 2004, 6, 4407–4410. [PubMed: 15548037]

(47). Hubert P; Heitzmann A; Viel S; Nicolas A; Sastre-Garau X; Oppezzo P; Pritsch O; Osinaga E; Amigorena S Antibody-dependent cell cytotoxicity synapses form in mice during tumor-specific antibody immunotherapy. Cancer Res. 2011, 71, 5134–5143. [PubMed: 21697279]

(48). Brode S; Cooke A Immune-potentiating effects chemo-therapeutic drug of the cyclophosphamide. Crit. Rev. Immunol 2008, 28, 109–126. [PubMed: 18540827]

(49). Liu P; Jaffar J; Hellstrom I; Hellstrom KE Administration of cyclophosphamide changes the immune profile of tumor-bearing mice. J. Immunother 2010, 33, 53–59. [PubMed: 19952956]

(50). Bachmann MF; Rohrer UH; Kundig TM; Burki K; Hengartner H; Zinkernagel RM The influence of antigen organization on B cell responsiveness. Science 1993, 262, 1448–1451. [PubMed: 8248784]

(51). Akache B; Weeratna RD; Deora A; Thorn JM; Champion B; Merson JR; Davis HL; McCluskie MJ Anti-IgE Qβ-VLP Conjugate Vaccine Self-Adjuvants through Activation of TLR7. Vaccines 2016, 4, 3.

(52). Jegerlehner A; Wiesel M; Dietmeier K; Zabel F; Gatto D; Saudan P; Bachmann MF Carrier induced epitopic suppression of antibody responses induced by virus-like particles is a dynamic phenomenon caused by carrier-specific antibodies. Vaccine 2010, 28, 5503–5512. [PubMed: 20307591]

(53). Yin Z; Chowdhury S; McKay C; Baniel C; Wright WS; Bentley P; Kaczanowska K; Gildersleeve JC; Finn MG; BenMohamed L; Huang X Significant impact of immunogen design on the diversity of antibodies generated by carbohydrate-based anti-cancer vaccine. ACS Chem. Biol 2015, 10, 2364–2372. [PubMed: 26262839]

(54). Dagan R; Poolman J; Siegrist C-A Glycoconjugate vaccines and immune interference: A review. Vaccine 2010, 28, 5513–5523. [PubMed: 20600514]

(55). Pobre K; Tashani M; Ridda I; Rashid H; Wong M; Booy R Carrier priming or suppression: Understanding carrier priming enhancement of anti-polysaccharide antibody response to conjugate vaccines. Vaccine 2014, 32, 1423–1430. [PubMed: 24492014]

(56). Luthe DS A simple technique for the preparation and storage of sucrose gradients. Anal. Biochem 1983, 135, 230–232. [PubMed: 6670744]

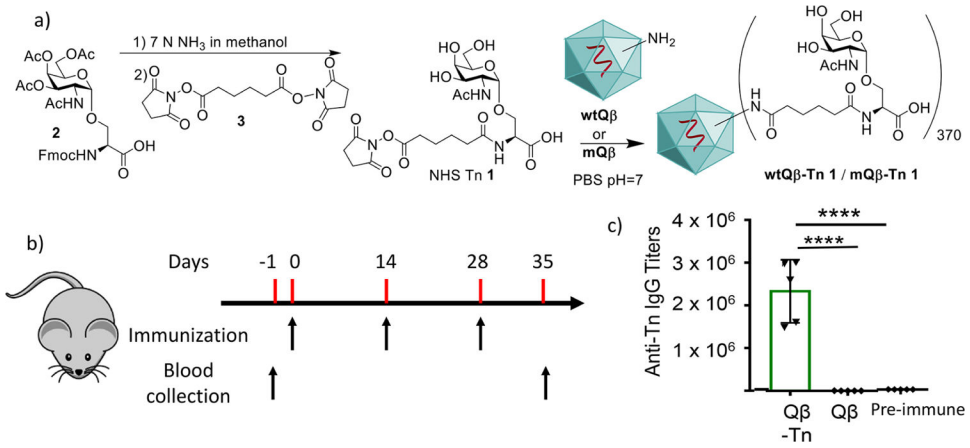

Figure 1.

Qβ is a powerful carrier to generate anti-Tn IgG antibody responses. (a) Synthesis of NHS Tn **1** and its conjugation with Qβ. (b) Mice were immunized with Qβ-Tn (1.9 μg of Tn per injection) and Qβ on days 0, 14, and 28. Blood was collected on days −1 and 35. (c) The titers of anti-Tn IgG antibodies in the sera on day 35 were analyzed from immunized mice by ELISA against the BSA-Tn conjugate. Preimmune refers to blood collected on day −1. Statistical analysis was performed using the Student *t* test by GraphPad Prism. ****$p <$ 0.0001.

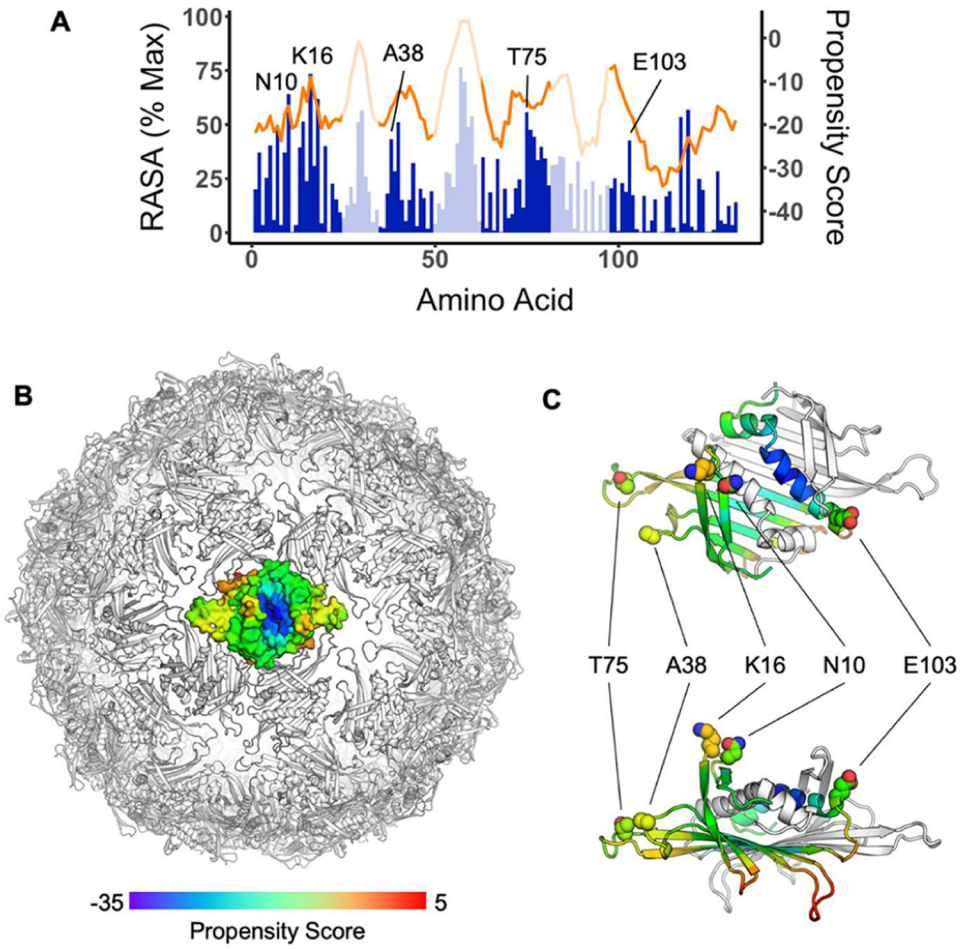

Figure 2.

(A) Relative accessible surface area (RASA, blue) and DiscoTope 2.0 propensity scores (orange) of residues from the Qβ coat protein sequence. Data represent the average of all three chains of the asymmetric unit. Regions facing the exterior of the VLP based on crystal structure analysis are shaded in dark blue color. (B) Propensity scores mapped by color onto coat protein dimer in the context of the full particle based on the particle crystal structure (PDB code 7TJM). Red indicates residues with higher B-cell epitope potential, while blue represents residues with lower B-cell epitope potential. (C) Close-up view of a dimer indicates the locations of surface-exposed and high B-cell propensity residues studied in this work.

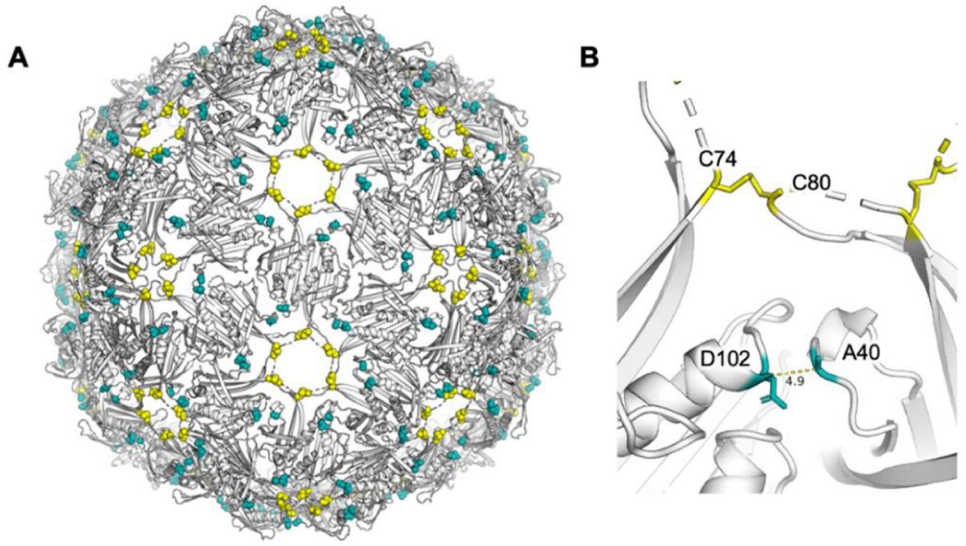

Figure 3.

X-ray crystal structure of Qβ (PDB code 7TJM) showing (A) disulfide bond networks from native disulfide bonds between C74 and C80 (yellow spheres) and the potential disulfide bond-forming residues in mQβ A40C/D102C (teal spheres). (B) Residues A40 and D102 are close to each other in the 3D structure of wtQβ, serving as potential sites for mutations to cysteines and the formation of an additional disulfide bond.

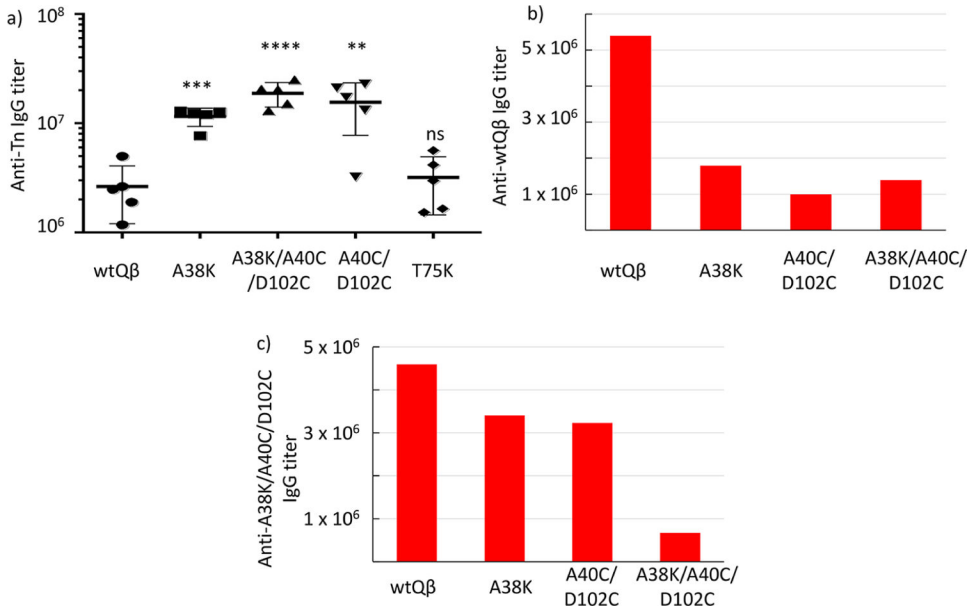

Figure 4.

(a) Anti-Tn IgG titers of postimmunized sera (day 35) from groups of mice ($n = 5$) vaccinated with various mQβ-Tn conjugates assayed against BSA-Tn as the coating antigen for ELISA. The statistical significance between a mQβ and wtQβ was determined by the Student t test using GraphPad Prism (**$p < 0.01$; ***$p < 0.001$; ****$p < 0.0001$; ns, not significant). Titers of (b) anti-wtQβ and (c) anti-mQβ(A38K/A40C/D102C) IgG antibodies in postimmunized sera (day 35) from groups of mice ($n = 5$) vaccinated with wtQβ, mQβ(A38K), mQβ(A40C/D102C), and mQβ(A38K/A40C/D102C) conjugates, respectively. The mQβ(A38K/A40C/D102C)-Tn conjugate induced higher titers of anti-Tn IgG antibodies with reduced antibody responses against both wtQβ and mQβ(A38K/A40C/D102C).

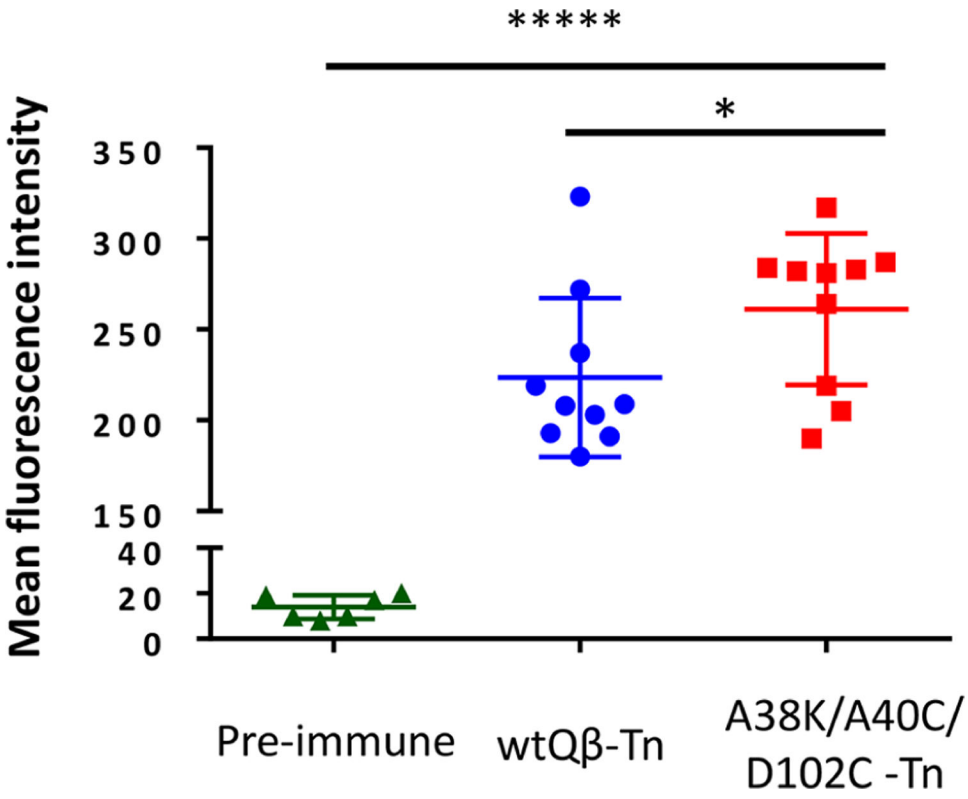

Figure 5.

Flow cytometry analysis showed stronger binding to TA3Ha cells by IgG antibodies elicited by the mQβ-Tn conjugate as compared to those by the wtQβ-Tn. The statistical significance was determined by the Student *t* test using GraphPad Prism (*$p < 0.05$; *****$p < 0.00001$).

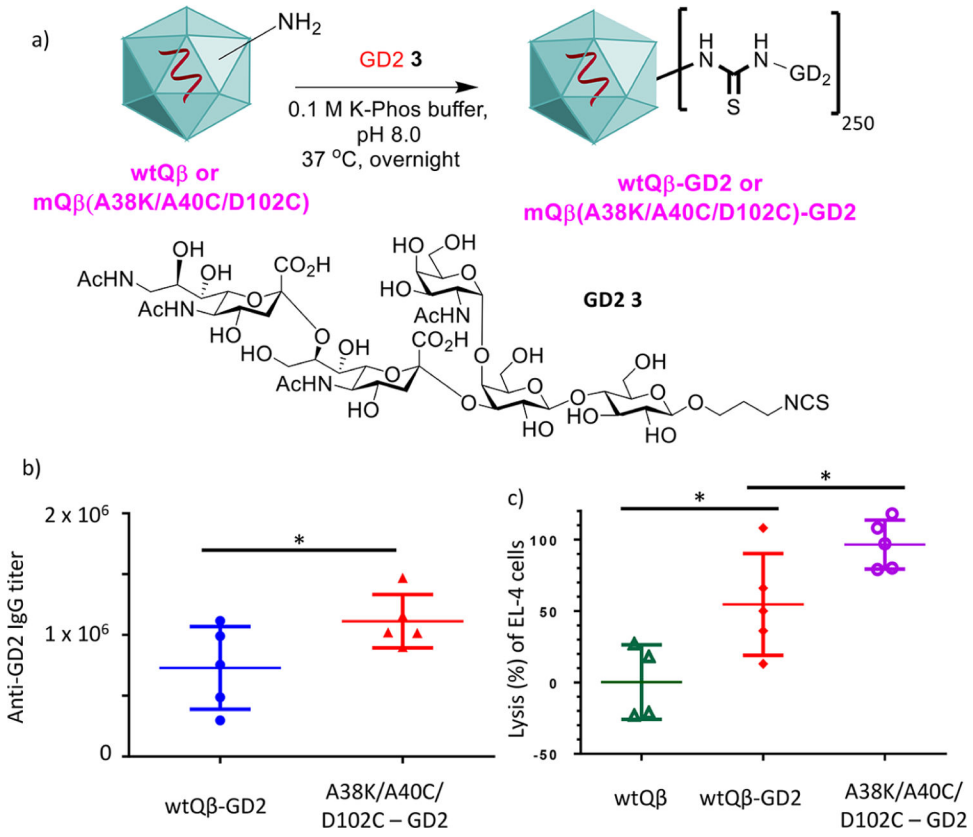

Figure 6.

(a) Synthesis of Q*β*-GD2 conjugates. Sera from mQ*β*-GD2 conjugate (b) elicited significantly higher anti-GD2 IgG antibody titers, and (c) exhibited significantly higher complement mediated cytotoxicity toward tumor cells compared with those of the corresponding wtQ*β*-GD2 conjugate. CDC toward EL4 cells was determined by the MTS assay. Each symbol represents one mouse ($n = 5$ mice for each group). *$p < 0.05$. The p values were determined through a two tailed t test using GraphPad Prism.

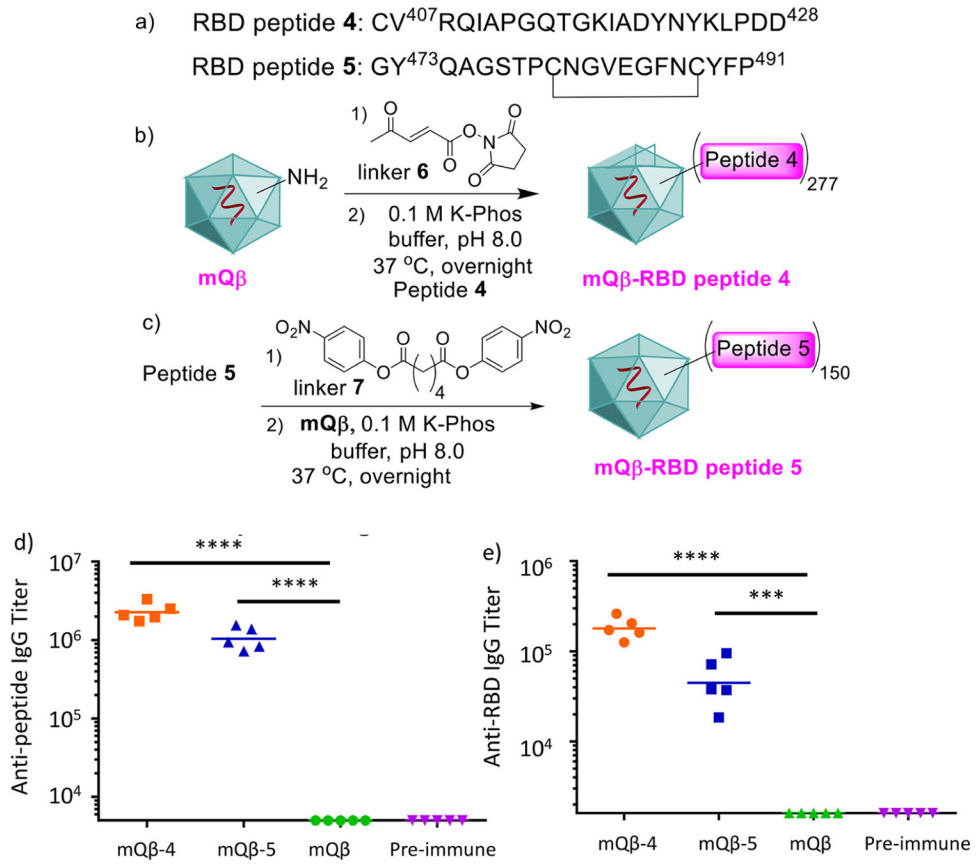

Figure 7.

(a) Sequences of RBD peptides **4** and **5**. (b) Synthesis of mQ*β*-RBD peptide **4** conjugate. (c) Synthesis of mQ*β*-RBD peptide **5** conjugate. mQ*β* is a powerful carrier to generate anti-SARS-CoV-2 IgG immune responses against (d) RBD peptides **4** and **5** and (e) the full RBD. Preimmune refers to blood collected on day −1. Statistical analysis was performed using the Student *t* test by GraphPad Prism. ***$p < 0.001$; ****$p < 0.0001$.

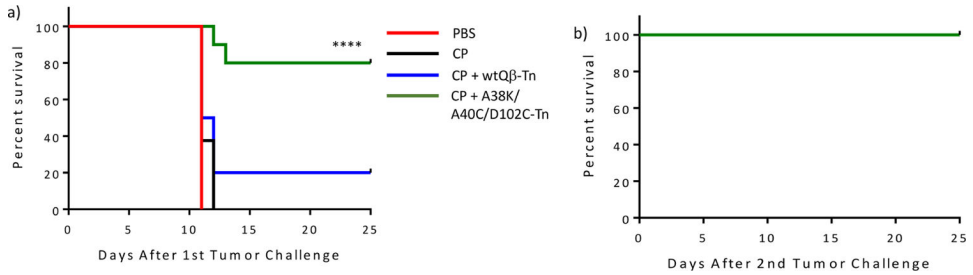

Figure 8.

(a) Vaccination with mQβ-Tn significantly improved the survival of mice as compared to those immunized with wtQβ-Tn in combination with CP chemotherapy. Groups of mice (n = 10 for each group) were intraperitoneally injected with 10 000 TA3Ha cells on day 0, with or without intraperitoneal treatment of cyclophosphamide (50 mg kg^{-1}) on day 1. wtQβ-Tn, or mQβ(A38K/A40C/D102C)-Tn formulated with MPLA (20 μg) as an adjuvant, was administrated intraperitoneally on days 1, 4, and 8, respectively. Statistical analysis of survival was performed with GraphPad Prism using the log-rank test comparing the mQβ(A38K/A40C/D102C)-Tn and the wtQβ-Tn groups. **** $p < 0.0001$. (b) Mice surviving tumor challenge from the CP/mQβ(A38K/A40C/D102C)-Tn group were rechallenged with TA3Ha cells. All mice survived without any further treatments.